NUKLEONIKA 2018;63(1):17–22
doi: 10.1515/nuka-2018-0003

ORIGINAL PAPER

Np-237 incineration study in various beams in ADS setup QUINTA

Stanisław Kilim, Elżbieta Strugalska-Gola, Marcin Szuta, Marcin Bielewicz, Sergej I. Tyutyunnikov, Walter I. Furman, Jindra Adam, Vladimir I. Stegailov

Abstract. Neptunium-237 samples were irradiated in a spallation neutron field produced in accelerator-driven system (ADS) setup QUINTA. Five experiments were carried out on the accelerators at the JINR in Dubna – one in carbon (C6+), three in deuteron, and one in a proton beam. The energy in carbon was 24 GeV, in deuteron 2, 4 and 8 GeV, respectively, and 660 MeV in the proton beam. The incineration study method was based on gamma-ray spectrometry. During the analysis of the spectra several fission products and one actinide were identified. Fission product activities yielded the number of fissions. The actinide (Np-238), a result of neutron capture by Np-237, yielded the number of captures. The main goal of this work was to find out if and how the incineration rate depended on parameters of the accelerator beam.

Keywords: Np-237 • accelerator-driven system (ADS) • gamma-ray spectrometry • fission • neutron capture

S. Kilim✉, E. Strugalska-Gola, M. Szuta, M. Bielewicz
National Centre for Nuclear Research
Andrzeja Sołtana 7, 05-400 Otwock-Świerk, Poland
E-mail: stanislaw.kilim@ncbj.gov.pl

S. I. Tyutyunnikov, W. I. Furman, J. Adam,
V. I. Stegailov
Joint Institute for Nuclear Research
Joliot-Curie 6, 141980 Dubna, Russia

Received: 28 June 2016
Accepted: 22 May 2017

Introduction

Neptunium is one of 15 actinides produced artificially in power reactors as a by-product of energy production. Np-237 is its longest-lasting isotope with a half-life of 2.144×10^6 y [1]. To eliminate its long-lasting activity one has to split it somehow. There is no easy way to achieve this. There are two possibilities of neutron interaction with Np-237 – fission and radiative capture – see Eq. (1). Np-237 nuclear fission leads to the production of two new isotopes of masses statistically dispersed around two maxima. Some isotopes, also known as fission products (FP), are produced directly from Np-237 fission and the others indirectly, as a result of the other route of fission product decay. The radiative neutron capture yields β^--active Np-238 nuclei. Formulae (3)–(7) show the production of Np-237 fission products and decay chains identified by gamma lines.

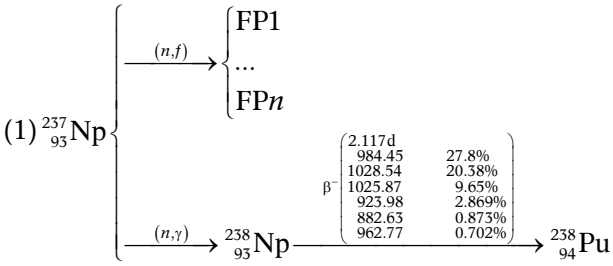

As shown in Fig. 1 the radiative neutron capture is a dominant way of interaction with neutrons in

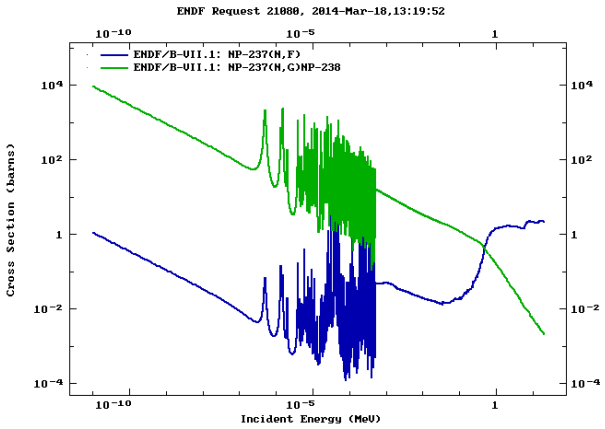

Fig. 1. Np-237 neutron-caused fission (blue) and capture (green) cross section dependence on energy [2].

the energy range 0–1 MeV. This is particularly important since the thermal region of neutron energy is the most available in present-day power reactors. Neutron capture induces the production of other actinides. As the nuclear fission of actinides releases about 170 MeV with fission product kinetic energy and about 7.5 MeV as prompt gamma quanta energy, while the radiative capture yields the energy in gamma quanta form only, capturing instead of fission results in the loss of energy. The newly produced actinides affect the neutron balance so much that a fuel campaign is shortened. A neutron energy region exists, at approximately 1 MeV and above, where fission of Np-237 dominates the radiative capture. That is why a nuclear power plant has to be based on fast reactors. Another concept of preventing/eliminating long-lasting activity/actinides is the accelerator-driven system (ADS) used for incineration.

In the ADS designs currently considered for industrial applications, such as EFIT (European Facility for Industrial Transmutation), the neutron spectrum is determined mainly by the isotopic composition and geometry of the system, not by the spectrum of the neutrons produced in the target.

As the geometry and isotopic composition of QUINTA was the same in each experiment, it is reasonable to expect its neutron spectrum to exhibit the same shape in each case, i.e. to be dominated by a U-238 fission spectrum. This means the fission-to-capture ratio should not depend on particles of beams nor their energies, at least not over the energy interval investigated here.

The Np-237 incineration results presented here are from experiments carried out in ADS-type setup QUINTA at JINR in Dubna, Russia. Table 1 shows the data of each experiment. Some results presented in this work – the ones from deuteron beams – have already been published in [3]. The new results are from a 660 MeV proton beam and a C6+ beam.

Experiment and data work out description

The core of the QUINTA setup (Fig. 2) consisted of aluminium-cladded elements of natural uranium arranged in five hexagonal sections. The total weight of the uranium was 500 kg. The uranium core was surrounded by a 10 cm-thick lead shield. For more details of the QUINTA setup construction see [4]. An accelerated beam of carbon ions (C6+), deuterons or protons impinged on the uranium core causing nuclei spallation and the production of fast neutrons. The Np-237 sample was located in a side window about 20 cm from the axis of the beam. The spallation neutrons caused U-238 fission which generated a number of neutrons while converting into the Np sample. The Np-237 sample was formed of a disk 21 mm in diameter encapsulated in a U-shaped casing. The gamma spectrum of the sample was measured several times by a CANBERRA GR1819

Table 1. Experimental data

	Beam energy/particle*				
	0.66 GeV/p	2 GeV/d	4 GeV/d	8 GeV/d	24 GeV/C6+
Date	8 Nov 2014	4 Dec 2012	13 Dec 2012	22 Dec 2012	18 Dec 2013
Irradiation time [h]	5.72	6.27	9.35	16.17	22.8
Total number of beam particles	8.64×10^{14}	$3.052(9) \times 10^{13}$	$3.569(15) \times 10^{13}$	$1.390(8) \times 10^{13}$	1.75×10^{11}

*Particles: p – proton, d – deuteron, C6+ – carbon.

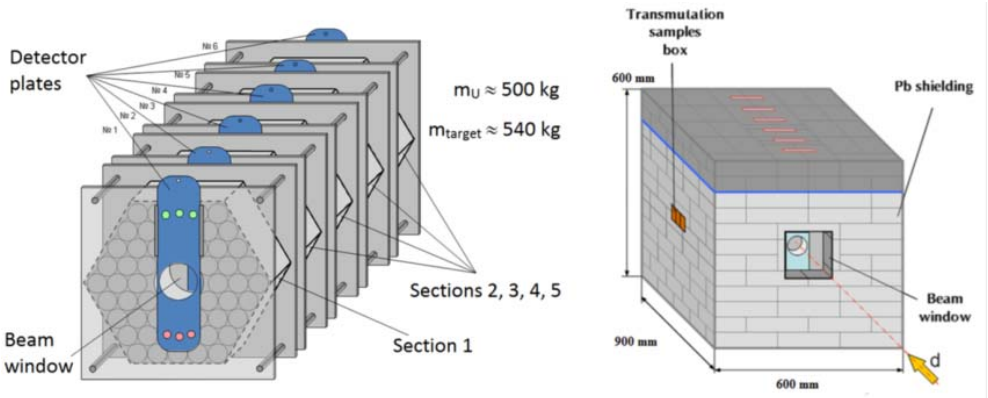

Fig. 2. QUINTA setup front view – internal core and outer lead shield.

spectrometer. The spectroscopy filters were made of Pb, Cd and Cu to reduce X-ray and low-energy gamma activity. Altogether it was composed of a 11.5 mm-thick Pb filter, in addition to 1 mm of Cd and 1 mm of Cu. Then, the following gamma spectra analysis aimed to identify gamma peaks as well as calculate their areas and parent isotopes. Co-60, Ba-133, Cs-137, Eu-152 and Th-228 samples were used as calibration sources for gamma spectrometer efficiency, ε_p. Generally some peaks stem from Np-237 fission products and the others from the neutron capture product, Np-238. The final measurements identified the number of Np-237 nuclei fissions and nuclei that absorbed neutrons. They were simply calculated from respective peak areas according to the formula:

$$(2)\qquad R_{f\gamma} = \frac{S_\gamma}{m\cdot\varphi\cdot\gamma_f\cdot\varepsilon_p\cdot I_\gamma}\cdot\frac{\lambda\cdot t_{\text{irr}}}{\left(1-e^{-\lambda\cdot t_{\text{irr}}}\right)}\cdot\frac{e^{\lambda\cdot t_+}}{\left(1-e^{-\lambda\cdot t_{\text{real}}}\right)}\cdot\frac{t_{\text{real}}}{t_{\text{live}}}$$

where: $R_{f\gamma}$ – actinide fission rate, per beam particle and per gram; γ – gamma line index; f – reaction index (f = fission); S_γ – gamma peak area; γ_f – isotope production yield [%]; m – activation sample mass [g]; ε_p – gamma spectrometer efficiency; I_γ – gamma line intensity [%]; φ – (deuteron/proton/C6+) integral number; λ – isotope decay constant; t_+ – cooling time; t_{irr} – irradiation time; t_{real} – real time of measurement; t_{live} – live time of measurement.

In the simplest case the isotopes produced directly from fission (like Sr-92, I-133 and I-135 – chain formulae (3), (4) and (5), respectively) or capture, and the beam intensity are constant. In the case of capture the formula is very similar to Eq. (2) except for the omitted γ_f coefficient. The simplicity of this case also means simple, exponential ($e^{\lambda\cdot t_+}$) correction to the cooling time.

$$(3)\quad \text{Fission}\xrightarrow{\gamma_1=4.01\%}{}^{92}_{38}\text{Sr}\xrightarrow{\beta^-\left(\begin{smallmatrix}2.71\text{h}\\1383.93\ \ 90\%\\953.31\ \ 3.52\%\\430.49\ \ 3.28\%\end{smallmatrix}\right)}{}^{92}_{39}\text{Y}\xrightarrow{\beta^-\left(\begin{smallmatrix}3.54\text{h}\\934.46\text{ keV }13.9\%\\1405.28\text{ keV }\ 4.8\%\\561.03\text{ keV }\ 2.4\%\\448.34\text{ keV }\ 2.34\%\\844.17\text{ keV }\ 1.25\%\end{smallmatrix}\right)}{}^{92}_{40}\text{Zr}$$

$$(4)\quad \text{Fission}\xrightarrow{\gamma=4.45\%}{}^{133}_{53}\text{I}\xrightarrow{\beta^-\left(20.8\text{h}\ 529.872\text{keV }87\%\right)}{}^{133}_{54}\text{Xe}\xrightarrow{\beta^-\left(5.243\text{d}\ 80.9971\text{keV }38\%\right)}{}^{133}_{55}\text{Cs}$$

$$(5)\quad \text{Fission}\xrightarrow{\gamma=4.16\%}{}^{135}_{53}\text{I}\xrightarrow{\beta^-\left(\begin{smallmatrix}6.57\text{h}\\1260.409\text{keV }28.9\%\\1131.511\text{keV }22.74\%\end{smallmatrix}\right)}{}^{135}_{54}\text{Xe}\xrightarrow{\beta^-\left(9.1\text{h}\ 249.77\text{keV }90\%\right)}{}^{135}_{55}\text{Cs}$$

There are some lines – like 658, 667, 772.6 and 954 keV – that behave in a more complicated way. Formulae (6) and (7) show respective isotope production/decay chains. The half-life of a parent isotope (like Zr-97) is characteristically much longer than that of a daughter isotope (Nb-97 in this case). After some time, i.e. following decay, this causes Nb-97 produced directly from fission to decay according to the half-life of Zr-97. Formula (8) takes these processes into account.

$$(6)\quad \left.\begin{array}{l}\text{Fission}\xrightarrow{\gamma_1=5.35\%}{}^{97}_{40}\text{Zr}\xrightarrow{\beta^-\left(\begin{smallmatrix}16.97\text{h}\\743.36\text{keV }93\%\\507.64\text{keV }\ 5.03\%\end{smallmatrix}\right)}\\ \text{Fission}\xrightarrow{\gamma_2=0.31\%}\end{array}\right\}\ {}^{97}_{41}\text{Nb}\xrightarrow{\beta^-\left(72.1\text{m}\ 658.08\text{keV }98\%\right)}{}^{97}_{42}\text{Mo}$$

$$(7)\quad \left.\begin{array}{l}\text{Fission}\xrightarrow{\gamma_1=3.98\%}{}^{132}_{52}\text{Te}\xrightarrow{\beta^-\left(\begin{smallmatrix}3.204\text{d}\\228.16\text{keV }88\%\\49.72\text{keV }15\%\end{smallmatrix}\right)}\\ \text{Fission}\xrightarrow{\gamma_2=0.407\%}\end{array}\right\}\ {}^{132}_{53}\text{I}\xrightarrow{\beta^-\left(\begin{smallmatrix}2.295\text{h}\\667.718\text{keV }99\%\\772.6\text{keV }\ 75.6\%\\954.55\text{keV }\ 17.6\%\end{smallmatrix}\right)}{}^{132}_{54}\text{Xe}$$

$$(8)\quad R_{f\gamma} = \frac{S_\gamma}{m\cdot\varphi\cdot\gamma_f\cdot\varepsilon_p\cdot I_\gamma}\cdot\frac{t_{\text{real}}}{t_{\text{live}}}\cdot\frac{t_{\text{irr}}}{\left[c_2\left(1-e^{-\lambda_2 t_{\text{real}}}\right)e^{-\lambda_2 t_+}+c_1\left(1-e^{-\lambda_1 t_{\text{real}}}\right)e^{-\lambda_1 t_+}\right]}$$

$$c_2 = \frac{\gamma_2}{\lambda_2}\left(1-e^{-\lambda_2 t_{\text{irr}}}\right)$$

$$c_1 = \frac{\gamma_1}{\lambda_1}\left(1-e^{-\lambda_1 t_{\text{irr}}}\right)$$

Table 2 shows all identified gamma lines and their data (isotope source, half-life, intensity and respective FP yield).

Data averaging was conducted over two steps – averaging over measurements for each isotope (Fig. 3) and then over isotopes or gamma lines in the capture case (Fig. 4).

Results

The results are presented in a selective way to illustrate each work out stage.

The left-hand side of Fig. 3 shows the fission rate of Np-237 (y axis) based on I-135 gamma lines from the 0.66 GeV/p experiment as a function of cooling time (x axis). The right-hand side shows the radiative capture rate of Np-237 based on the activity of the 984 keV line vs. cooling time. Punctual marks represent the results of one measurement. The solid line represents an average value while the dashed lines represent the $\pm\sigma$ (standard deviation) range. The errors include statistical and detector efficiency components (10%).

Figure 4 shows the rates of Np-237 fission (left side) and radiative capture (right side) for the next work out stage. Punctual marks represent average values for one isotope (FP) or gamma line (capture). The error value corresponds to σ from Fig. 3. The solid line represents the average value, averaged over all isotopes – the left-hand side case, or gamma lines – the right-hand side one. Dashed lines represent the $\pm\sigma$ (standard deviation) range.

Table 2. Sample Np-237-identified gamma lines and their data

E-gamma [keV]	Isotope	Source	$T_{1/2}$	Fission yield [%] [5]	I-gamma [%] [6]
529.87	^{133}I	FP	20.87 h	4.45	87.0
658.08	^{97}Nb*	FP	16.744 h	5.38	98.23
667.71	^{132}I**	FP	3.26 d	4.39	98.7
743.36	^{97}Zr	FP	16.744 h	5.35	93.6
772.60	^{132}I**	FP	3.26 d	4.39	75.6
954.55	^{132}I**	FP	3.26 d	4.39	17.6
1131.51	^{135}I	FP	6.57 h	4.16	22.6
1260.41	^{135}I	FP	6.57 h	4.16	28.7
1383.93	^{92}Sr	FP	2.66 h	4.01	90.0
923.98	^{238}Np	CP	2.117 d	N/A	2.869
962.77	^{238}Np	CP	2.117 d	N/A	0.702
984.45	^{238}Np	CP	2.117 d	N/A	27.8
1025.87	^{238}Np	CP	2.117 d	N/A	9.65
1028.54	^{238}Np	CP	2.117 d	N/A	20.38

FP – fission product. CP – neutron capture product.
* Nb-97 quantity and decay rate is modified by its parent isotope Zr-97.
** I-132 quantity and decay rate is modified by its parent isotope Te-132.

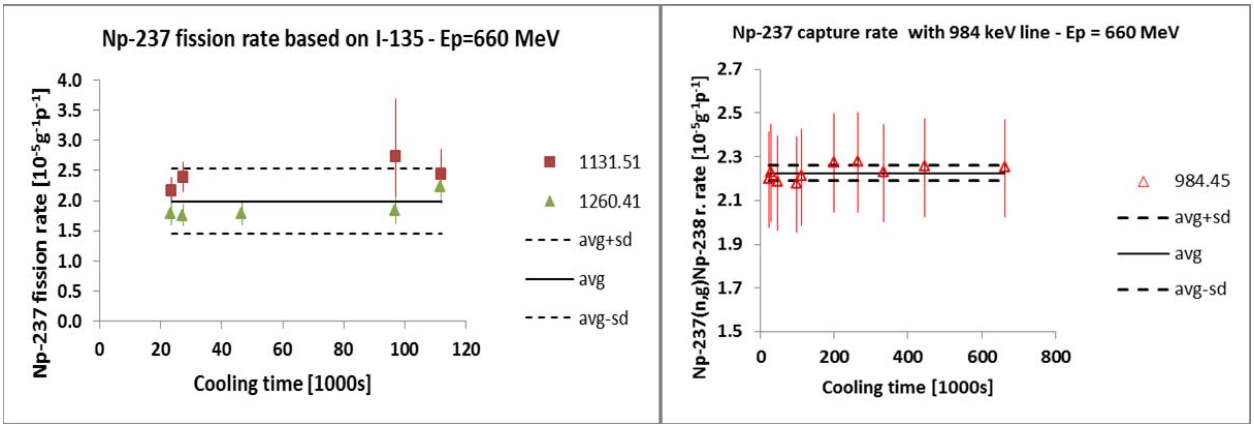

Fig. 3. Np-237 fission and capture results shown on I-135 lines and Np-238 gamma line of 984 keV (experiment 0.66 GeV/p).

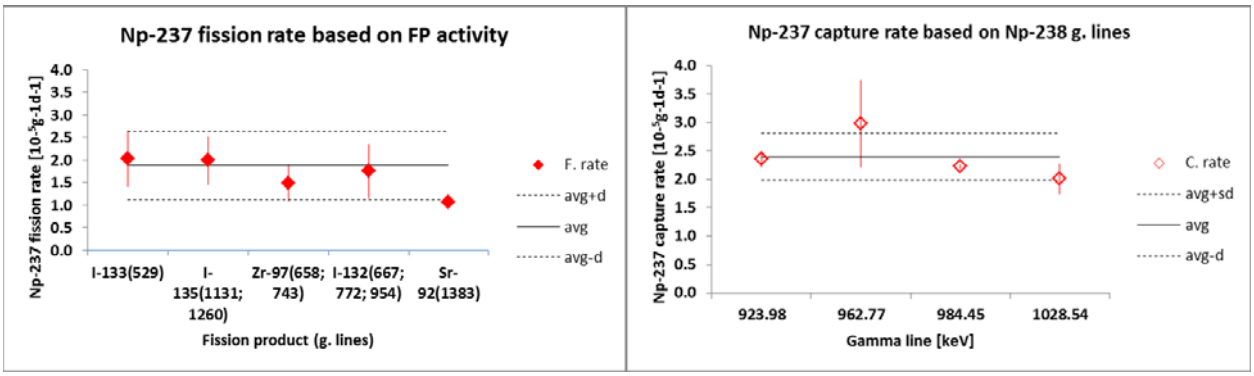

Fig. 4. Np-237 fission and capture rate results (experiment 0.66 GeV/p).

Figure 5 shows the number of Np-237 fissions and captures – top-left – "bare" results (per gram of sample and one beam particle), top-right – the previous ones per (ion) nucleon, bottom-left – the previous ones per (ion) energy unit, bottom-right – the top-left ones per proton and per (ion) energy unit. Legend – reaction/particle – for example F/p – fission/proton. X-axis shows ion energy in GeV.

Figure 6 shows the fission-to-capture ratio (F/C) for each experiment. Punctual marks represent the value of F/C for one experiment. Blue triangles (Zav-f/c) represent data derived from [7]. Experiment mnemonics are shown as x axis symbols. A summary of the results is shown in Table 3. The fission-to-capture ratio seems to be the most appropriate parameter for analysis because division eliminates some possible common errors.

The results of the five experiments identified which ion and which energy level is the most appropriate for Np-237 incineration, and the general incineration of actinides. Figure 5 is helpful in this regard. First, the reaction rate must be related to

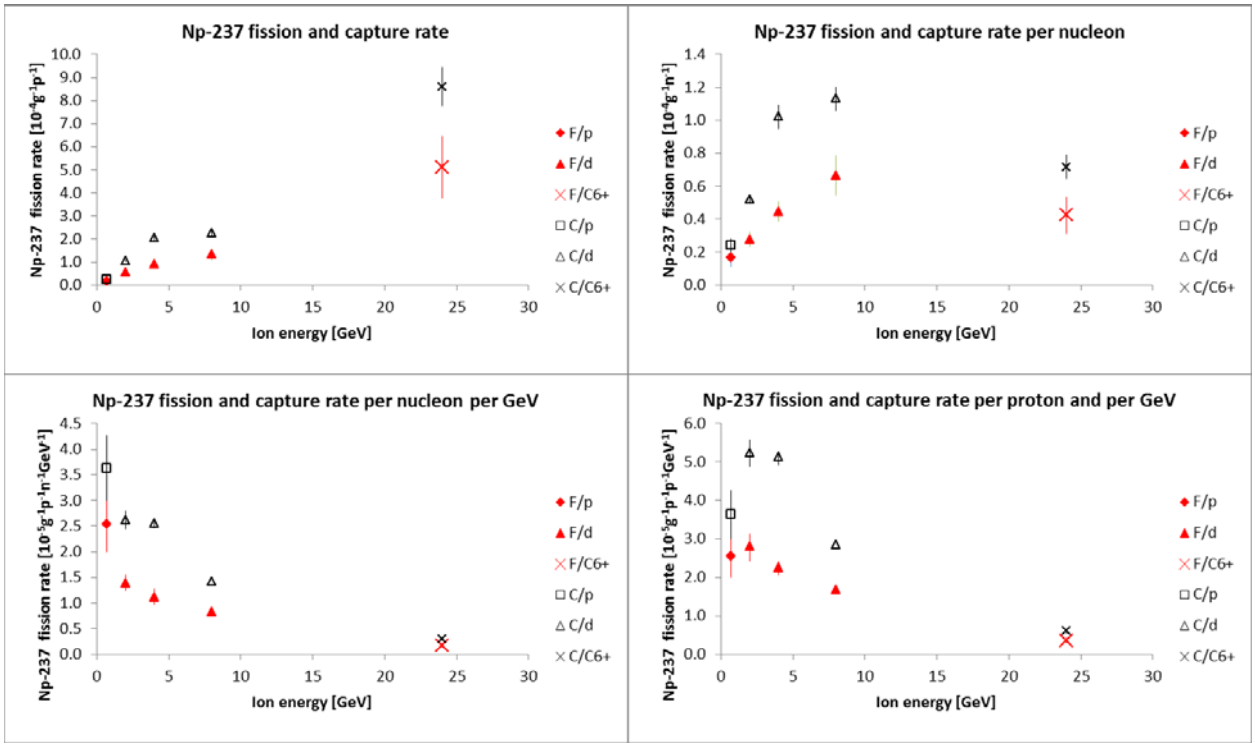

Fig. 5. Np-237 fission and capture rate results and their successive recalculation; top-left – "bare" results (per sample gram and one beam particle), top-right – the previous ones per one (ion) nucleon, bottom-left – the previous ones per ion energy unit, bottom-right – top-left ones per proton and per ion energy unit.
Legend – reaction/particle – for example F/p – fission/proton.

the mass of the sample and to one beam ion particle – Fig. 5 top-left. Then it must be related to one ion nucleon and one unit of energy – GeV – Fig. 5 bottom-left. According to this analysis the proton is the most effective in Np-237 incineration. Nevertheless, the results from deuteron are disturbing. The effectiveness of the proton is approximately twice as big as that of deuteron. It looks like the energy brought into the target by the neutron of deuteron is lost, i.e. the neutron does not produce spallation neutrons or at least produces them much less than the ion particle proton. Intuitively this is acceptable because a proton-target nucleus interaction, the electrical (+ nuclear) one, covers a much larger range than the neutron-nucleus one, the nuclear one. Therefore the specific incineration potential has been recalculated per ion particle proton, not per nucleon. It is believed these data outline the dependence of proton and deuteron incineration potential on ion energy. Figure 5 bottom-right shows 2 GeV deuteron effectiveness to be a little larger than that of the proton. The C6+ ions are much less effective than the proton and deuteron. The effectiveness of deuteron decreases with energy as expected, because the greater the energy the shorter the time of flight through the target nucleus. Generally, the incineration potential peaks when the energy of the deuteron beam is equal to 2 GeV.

As construction of the target was the same for each experiment the number of neutrons crossing the sample, i.e. number of fissions, should be proportional to the number of spallation neutrons. In spite of the different targets (uranium and lead) it can be stated that the behaviour of the results in

Table 3. Basic Np-237 incineration parameters for each experiment

Average fission and capture	Particle energy/particle				
	0.66 GeV/p	2 GeV/d	4 GeV/d	8 GeV/d	24 GeV/C6+
Fission (10^{-5} $g^{-1}\cdot p^{-1}$)	1.67(35)	5.56(87)	8.95(12)	13.3(24)	51.1(135)
Capture (10^{-5} $g^{-1}\cdot p^{-1}$)	2.40(42)	10.10(43)	20.40(14)	22.6(14)	86.1(84)
Fission (10^{-5} $g^{-1}\cdot p^{-1}\cdot nucleon^{-1}$)	1.67(35)	2.78(43)	4.47(60)	6.65(12)	4.26(11)
Capture (10^{-5} $g^{-1}\cdot p^{-1}\cdot nucleon^{-1}$)	2.40(42)	5.22(22)	10.21(71)	11.31(7)	7.17(7)
Fission (10^{-5} $g^{-1}\cdot p^{-1}\cdot nucleon^{-1}\cdot GeV^{-1}$)	2.53(53)	1.39(22)	1.12(15)	0.83(15)	0.18(5)
Capture (10^{-5} $g^{-1}\cdot p^{-1}\cdot nucleon^{-1}\cdot GeV^{-1}$)	3.63(63)	2.61(11)	2.55(18)	1.41(9)	0.30(3)
Fission (10^{-5} $g^{-1}\cdot p^{-1}\cdot proton^{-1}\cdot GeV^{-1}$)	2.53(53)	2.78(43)	2.24(30)	1.66(30)	0.35(9)
Capture (10^{-5} $g^{-1}\cdot p^{-1}\cdot proton^{-1}\cdot GeV^{-1}$)	3.63(63)	5.22(22)	5.11(35)	2.83(18)	0.60(6)
F/C	0.70(19)	0.53(9)	0.44(7)	0.59(11)	0.59(17)
F/A	0.41(11)	0.35(6)	0.30(5)	0.37(7)	0.37(11)

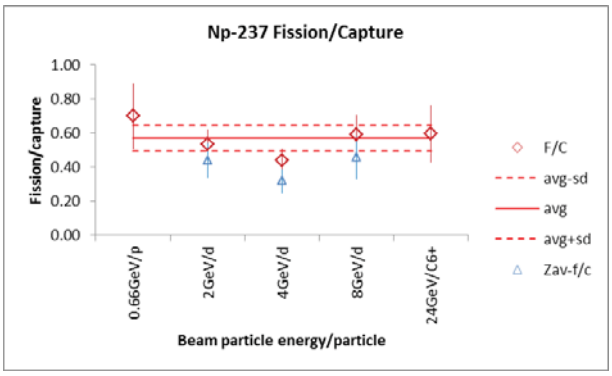

Fig. 6. Np-237 fission-to-capture ratio for each experiment.

the bottom-right of Fig. 5 agrees in general with Hashemi-Nezhad [8] – (Fig. 2. Neutron/GeV dependence on ion energy).

It is not clear why the capture rate behaves a little differently to the fission one. As shown in Fig. 6, the fission-to-capture ratio deviates from its average value of 0.57(8) by more than statistics allow. According to statistics 68.27% of results should fall within $\pm\sigma$ (2 standard deviations) but only 60% fall within this range in this experiment.

Conclusions

Five experiments were carried out using a QUINTA-ADS-type setup to investigate the incineration potential of Np-237. The ion beam consisted of protons (0.66 GeV), deuterons (2, 4 and 8 GeV) and carbon C6+ (24 GeV).

Beam ion particle neutrons are thought not to contribute or contribute much less than protons to the incineration of Np-237.

The most appropriate parameters of comparison were the number of fissions per gram of sample material, per beam ion particle, per beam ion particle proton, and per beam energy unit.

It was found that deuterons possessing approximately 2 GeV of energy exhibit the biggest incineration potential related to beam ion particle proton. The heavier ions are less effective in terms of Np-237 incineration.

The dependence of neutron capture on ion energy is different to that of fission.

The fission-to-capture (F/C) and fission-to-absorption (F/A) ratios are the other parameters that characterize the effectiveness of incineration.

In each experiment the fission-to-capture ratio of Np-237 was less than 1, i.e. actinides still cumulate in QUINTA.

The fission-to-capture ratio deviates from its expected average value by more than statistics allow. 60% of results fall within $\pm\sigma$ (2 standard deviations) instead of 68.27%.

Acknowledgments. The authors would like to thank the staff of the Nuclotron and Phasotron Accelerators at the Joint Institute for Nuclear Research in Dubna, Russia for providing access to the research facilities used in these experiments.

References

1. Chu, S. Y. F., Ekström, L. P., & Firestone, R. B. (1999, February). The Lund/LBNL Nuclear Data Search. Version 2.0. Retrieved from http://nucleardata.nuclear.lu.se/toi/listnuc.asp?sql=&Z=93.
2. Evaluated Nuclear Data File (ENDF). Vienna, International Atomic Energy Agency. Retrieved March 18, 2014, from https://www-nds.iaea.org/exfor/endf.htm.
3. Kilim, S., Bielewicz, M., Strugalska-Gola, E., Szuta, M., Furman, W. I., Tyutyunnikov, S., Adam, J., Zavorka, L., Khushvaktov, J., Kish, Yu., Tsoupko-Sitnikov, V. M., Solnyshkin, A. A., & Vrzalova, J. (2015). Measurements of Np-237 incineration in ADS setup QUINTA. XXII International Baldin Seminar on High Energy Physics Problems, 15–20 September 2014, JINR, Dubna, Russia. *PoS(Baldin ISHEP XXII)056.*
4. Furman, W., Adam, J., Balwin, A., Gundorin, N., Hushvaktov, Zh., Kadykov, M., Kopatch, Zh., Kostyukhov, E., Kudashkin, I., Makan'kin, A., Mar'in, I., Polansky, A., Pronskikh, V., Rogov, A., Schegolev, V., Solnyshkin, A., Tsupko-Sitnikov, V., Tyutyunnikov, S., Vishnevsky, A., Vladimirova, N., Wojciechowski, A., Zavorka, L., Chilap, V., Chinenov, A., Dubinkin, B., Fonarev, B., Galanin, M., Kolesnikov, V., Solodchenkova, S., Artyushenko, M., Sotnikov, V., Voronko, V., Khilmanovich, A., Martsynkevich, B., Kislitsin, S., Kvochkina, T., Zhanov, S., Husak, K., Korneev, S., Potapenko, A., Safronova, A., Zhuk, I., Suchopar, M., Svoboda, O., Vrzalova, J., Wagner, V., Kostov, L., Stoyanov, Ch., Zhivkov, P., Bielevicz, M., Kilim, S., Strugalskas-Gola, E., Szuta, M., Westmeier, W., Manolopoulou, M., & Hashemi-Nezhad, S. R. (2013). Recent results of the study of ADS with 500 kg natural uranium target assembly QUINTA irradiated by deuterons with energies from 1 to 8 GeV at JINR NUCLOTRON. XXI International Baldin Seminar on High Energy Physics Problems, 10–15 September 2012, JINR, Dubna, Russia. *PoS(Baldin ISHEPP XXI)086.*
5. Evaluated Nuclear Data File (ENDF). Interpreted ENDF file. NP-237(FY_cum)NP-238,RNP MAT=9346 MF=8 MT=459 Library: ENDF/B-VII.1. (n,FY_cum) Cumulative Fission-Product Yields and (n,ind_FY) Independent Fission-Product Yields. Retrieved from https://www-nds.iaea.org/exfor.endf.htm.
6. *Table of Isotopes, 8E* (8th ed.). (1999 update). [CD-ROM].
7. Zavorka, L., Adam, J., Baldwin, A. A., Caloun, P., Chilap, V. V., Furman, W. I., Kadykov, M. G., Khushktov, J., Pronskikh, V. S., Solnyshkin, A. A., Sotnikov, V., Stegailov, V. I., Suchopar, M., Tsoupko-Sitnikov, V. M., Tyutyunnikov, S. I., Voronko, V., & Vrzalova, J. V. (2015). Neutron-induced transmutation reactions in ^{237}Np, ^{238}Pu, and ^{239}Pu at the massive natural uranium spallation target. *Nucl. Instrum. Methods Phys. Res. Sect. B-Beam Interact. Mater. Atoms*, *349*, 31–38. DOI: 10.1016/j.nimb.2014.12.084.
8. Hashemi-Nezhad, S. R., Westmeier, W., Zamani-Valasiadou, M., Thomauske, B., & Brandt, R. (2011). Optimal ion beam, target type and size for accelerator driven systems: Implications to the associated accelerator power. *Ann. Nucl. Energy*, *38*(5), 1144–1155.